SAND2017-11126R

Finite Element in Angle Unit Sphere Meshing for Charged Particle Transport

Mario I. Ortega[a], Clif R. Drumm[a]

[a]*Sandia National Laboratories, Radiation Effects Theory Department*
P.O. Box 5800, MS1179, Albuquerque, New Mexico 87185

[*]morteg@sandia.gov

Number of pages: 19

Number of tables: 2

Number of figures: 14

Abstract

Finite element in angle formulations of the charged particle transport equation require the discretization of the unit sphere. In Sceptre, a three-dimensional surface mesh of a sphere is transformed into a two-dimensional mesh. Projection of a sphere onto a two-dimensional surface is well studied with map makers spending the last few centuries attempting to create maps that preserve proportion and area. Using these techniques, various meshing schemes for the unit sphere were investigated.

Keywords: Charge Particle Transport, Finite Element in Angle, Sphere Projection onto Surface

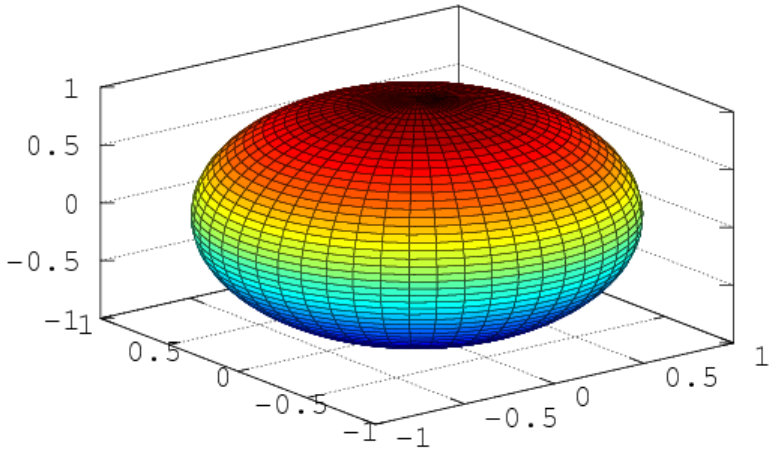

Fig. 1. Selection of Points on Unit Sphere

I. INTRODUCTION

This report details a study on the generation of finite element meshes for the unit sphere. Traditionally, transport methods have used the discrete ordinates approach to discretize the angular phase space. With the inclusion of electromagnetic fields, it is necessary to use a finite element approach in angle. The projection of a three-dimensional sphere surface onto a two-dimensional space is a well studied problem. Mapmakers throughout the centuries have attempted to use different projections to conserve distances and areas on the surface of sphere (in their case, the Earth). In this report, we study various of these projection schemes and apply them to a test problem found in the SCEPTRE code.

II. UNIT SPHERE MESHING SCHEMES

In this section we detail the meshing schemes used. We describe the nature of the projection, the projection equations, and show an example of the mesh created by the scheme. Points on the unit sphere we generated by using Octave's sphere command. The top hemisphere of the sphere was then selected and the points used to create the two-dimensional meshes that was later used in the test problem. The unit sphere created using this process is seen in Figure 1.

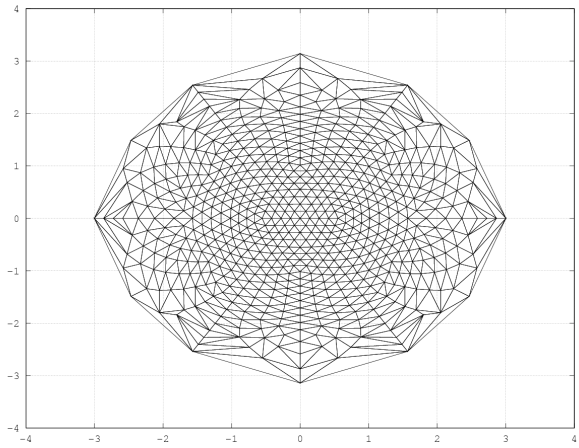

Fig. 2. Coarse Mesh of the Unit Sphere using Azimuthal Equidistant Projection of Unit Sphere

II.A. Azimuthal Equidistant Projection

A point on the sphere is selected such that mapped distances and azimuths from that point to any other point will be correct. The point on the sphere given by (θ, ϕ) is mapped to two-dimensional Cartesian space using the following relationships

$$x = \rho \sin\theta, \quad y = -\rho \cos\theta, \tag{1}$$

where ρ is the radius of the sphere (for the unit sphere $\rho = 1$). Figure 2 shows a coarse mesh projection of the unit sphere onto two-dimensional Cartesian space. As the projection is refined, the area of the projection becomes equal to 4π.

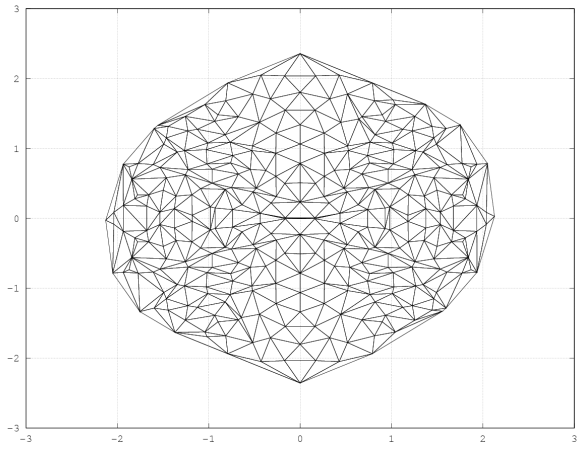

Fig. 3. Coarse Mesh using Bonne Projection of Unit Sphere

II.B. Bonne Projection

A Bonne projection is an equal-area projection. The projection transforms a point on the unit sphere surface, (θ, ϕ), onto a point, (x, y), on a two-dimensional Cartesian surface using the following equations

$$x = \rho \sin E, \quad y = \cot \phi_1 - \rho \cos E, \tag{2}$$

where

$$\rho = \cot \phi_1 + \phi_1 - \rho, \quad E = \frac{(\theta - \theta_0) \cos \phi}{\rho}. \tag{3}$$

The constants θ_0 and ϕ_1 are the angle of the central meridian and the standard parallel of the projection respectively. A coarse mesh projection of the unit sphere using the Bonne projection can be seen in Figure 3.

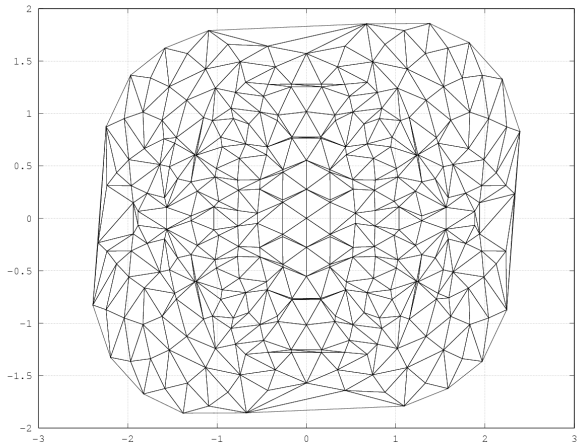

Fig. 4. Coarse Mesh of the Unit Sphere using Bottomley Projection of Unit Sphere

II.C. Bottomley Projection

The Bottomley projection is an equal area projection. The projection transforms a point on the unit sphere surface, (θ, ϕ), to a point on a two-dimensional Cartesian surface using the following equations

$$x = \frac{\rho \sin E}{\sin \phi_1}, \quad y = \frac{\pi}{2} - \rho \cos E, \tag{4}$$

where ρ and E are given by

$$\rho = \frac{\pi}{2} - \phi, \quad E = \frac{\theta \sin \phi_1 \sin \rho}{\rho}, \tag{5}$$

where ϕ_1 is the given parallel of the projection in radians. A coarse mesh projection of the unit sphere using the Bottomley projection can be seen in Figure 4.

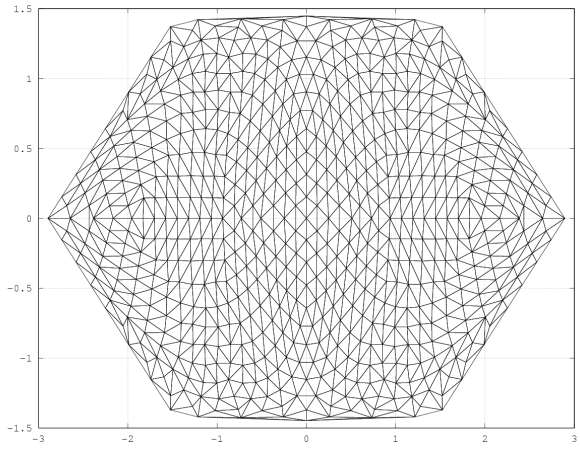

Fig. 5. Coarse Mesh of the Unit Sphere using Eckert II Projection of Unit Sphere

II.D. Eckert II Projection

The Eckert II projection is an equal area projection. The projection is symmetrical about the equator and central meridian of the unit sphere. The projection transforms a point on the unit sphere surface, (θ, ϕ), to a point on a two-dimensional Cartesian surface using the following equations

$$x = 2R(\theta - \theta_0)\sqrt{\frac{4 - 3\sin|\phi|}{6\pi}}, \quad y = \text{sign}(\phi)R\sqrt{\frac{2\pi}{3}}\left(2 - \sqrt{4 - \sin|\phi|}\right), \tag{6}$$

where θ_0 is the central meridian and R is the radius of the unit sphere. A coarse mesh projection of the unit sphere using the Eckert II projection can be see in Figure 5.

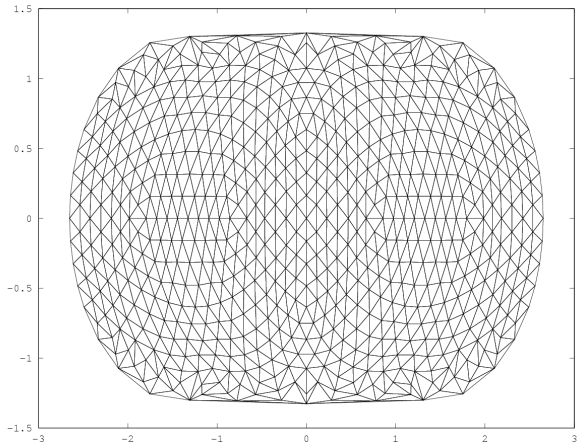

Fig. 6. Coarse Mesh of the Unit Sphere using Eckert IV Projection of Unit Sphere

II.E. Eckert IV Projection

The Eckert IV projection is an equal area projection. The projection takes the unit sphere and project it onto an ellipse. For points on the sphere with coordinates, (θ, ϕ), the projection onto the ellipse is given by

$$x = \frac{2}{\sqrt{4\pi + \pi^2}} R(\theta - \theta_0)(1 + \cos\alpha), \quad y = 2\sqrt{\frac{\pi}{4+\pi}} R \sin\alpha \tag{7}$$

where

$$\alpha + \sin\alpha\cos\alpha + 2\sin\alpha = \left(2 + \frac{\pi}{2}\right)\sin\phi. \tag{8}$$

α must be solved for numerically using a root finding method such as Newton's Method. Figure 6 shows a coarse mesh projection of the unit sphere using the Eckert II projection.

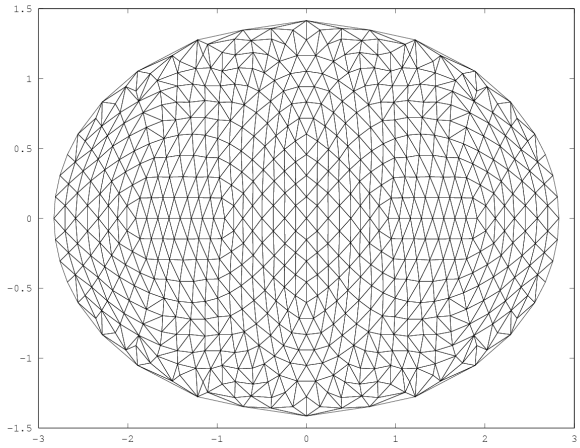

Fig. 7. Coarse Mesh of the Unit Sphere using Elliptical Projection of Unit Sphere

II.F. Elliptical Projection

The Elliptical projection (also knows as the Mollweide projection) projects the surface of the unit sphere onto an ellipse. The sphere is represented as a proportional 2:1 ellipse. The points located on the unit sphere, (θ, ϕ), are projected onto the ellipse using the following equations

$$x = R\frac{2\sqrt{2}}{\pi}(\theta - \theta_0)\cos\alpha, \quad y = R\sqrt{2}\sin\alpha, \tag{9}$$

where

$$2\alpha + \sin 2\alpha = \pi \sin\phi. \tag{10}$$

α must be solved for iteratively. If $\phi = \pm\frac{\pi}{2}$, then $\alpha = \pm\frac{\pi}{2}$ to avoid the possibility of division by zero. Figure 7 shows a coarse grid projection of the unit sphere.

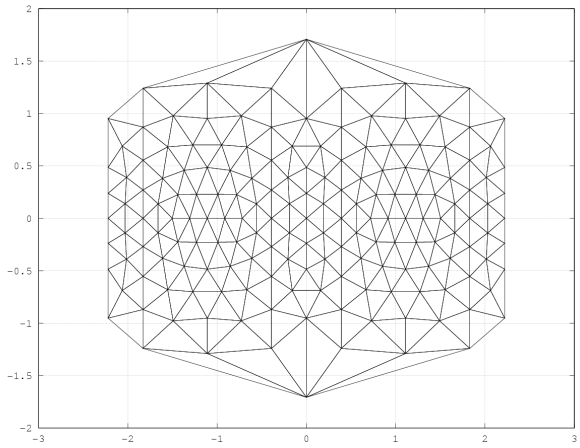

Fig. 8. Coarse Mesh of the Unit Sphere using Gall Stereographic Projection of Unit Sphere

II.G. Gall Stereographic Projection

The Gall stereographic projection is a projection that does preserve area or is conformal. The points on the unit sphere with coordinates (θ, ϕ) are transformed using the following equations

$$x = \frac{R\theta}{\sqrt{2}}, \quad y = R\left(1 + \frac{\sqrt{2}}{2}\right) \tan\frac{\phi}{2}, \tag{11}$$

where R is the radius of the sphere. Figure 8 shows a coarse grid projection of the unit sphere using Gall stereographic projection.

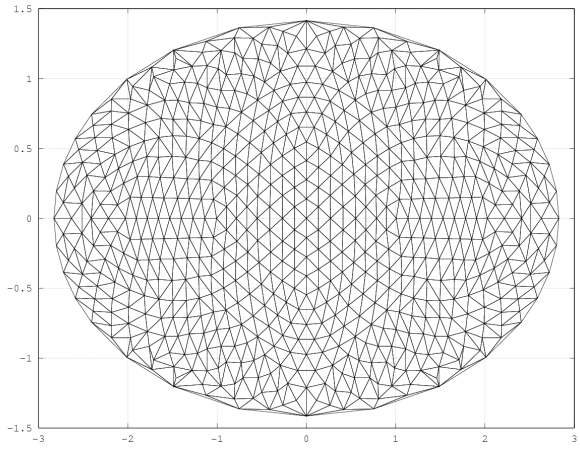

Fig. 9. Coarse Mesh of the Unit Sphere using Hammer Projection of Unit Sphere

II.H. Hammer Projection

The Hammer projection is an equal area projection. Points on the unit sphere (θ, ϕ) are transformed onto two-dimensional Cartersian space using the following equations

$$x = \text{laea}_x\left(\frac{\theta}{2}, \phi\right), y = \frac{1}{2}\text{laea}_y\left(\frac{\theta}{2}, \phi\right), \tag{12}$$

where we define the functions laea_x and laea_y as

$$\text{laea}_x\left(\frac{\theta}{2}, \phi\right) = \frac{2\sqrt{2}\cos\phi\sin\frac{\theta}{2}}{\sqrt{1+\cos\phi\cos\frac{\theta}{2}}}, \quad \text{laea}_y\left(\frac{\theta}{2}, \phi\right) = \frac{2\sqrt{2}\sin\phi}{\sqrt{1+\cos\phi\cos\frac{\theta}{2}}}. \tag{13}$$

Figure 9 shows a coarse grid projection of the unit sphere using Hammer projection.

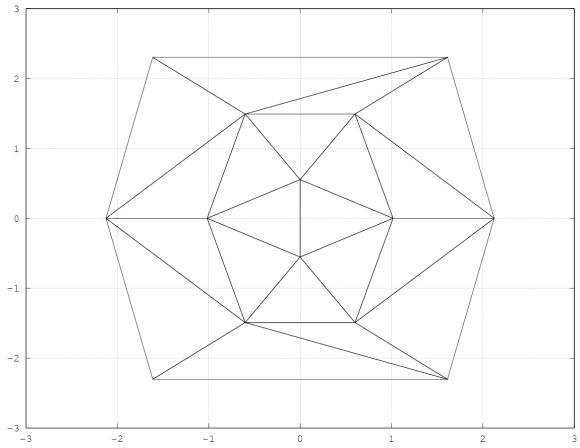

Fig. 10. Coarse Mesh of the Unit Sphere using Polyconic Projection of Unit Sphere

II.I. Polyconic Projection

Polyconic projection projects the unit sphere onto a circle. For points on the unit sphere given by (θ, ϕ), the projection is described by

$$x = \cot\phi\big((\theta - \theta_0)\sin\phi\big), \quad y = \phi - \phi_0 + \cot\phi\bigg(1 - \cos\big((\theta - \theta_0)\sin\phi\big)\bigg), \tag{14}$$

where θ_0 and ϕ_0 are the central meridian and the latitude chosen to be the origin at θ_0. If $\phi = 0$, then $x = \theta - \theta_0$ and $y = -\phi_0$ to avoid division by zero. Figure 10 shows a coarse unit sphere approximation using polyconic projection.

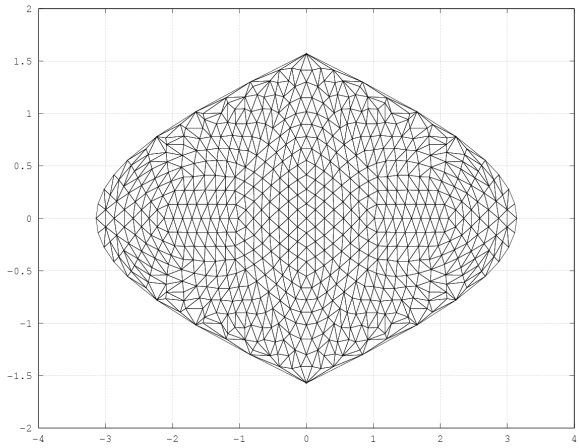

Fig. 11. Coarse Mesh of the Unit Sphere using Sinusoidal Projection of Unit Sphere

II.J. Sinusoidal Projection

Sinusoidal projection is an equal area projection. The projection is defined as

$$x = (\theta - \theta_0)\cos\phi, \quad y = \phi \tag{15}$$

where θ_0 is the central meridian. A coarse mesh of the unit sphere created using sinusoidal projection is seen in Figure 11.

TABLE I
Unit Sphere Projection Mesh Refinement Error Norms

N	Azimuthal Equidistant	Bonne	EckertII	EckertIV
5	3.37886	NaN	3.23727	NaN
10	1.74858	NaN	5.42324	4.19936
15	NaN	NaN	1.73128	NaN
20	NaN	NaN	1.40333	NaN
25	NaN	0.669671	0.904281	NaN
30	1.37466	2.45754	0.344995	0.818431

TABLE II
Unit Sphere Projection Mesh Refinement Error Norms

N	Elliptical	Gall Stereo	Hammer	Polyconic	Sinusoidal
5	NaN	4.72614	4.14842	NaN	10.024
10	6.6788	NaN	3.52743	7.02542	2.82338
15	2.16693	1.75353	4.36781	4.53914	4.93965
20	3.8455	NaN	NaN	NaN	1.66892
25	3.19011	NaN	1.48468	NaN	NaN
30	2.66479	NaN	0.943321	NaN	0.954384

III. RESULTS

A mesh refinement study was done using the various projection schemes to create two-dimensional meshes. N number of points on the unit sphere were selected and then transformed using the projection. The L2 norm of the numerical solution as compared to the analytical solution was used to compare the different refinement schemes. For various schemes, bad elements were created leading to disagreement with the analytical solutions. Further research might include the possibility of fixing bad elements. Sinusoidal and Eckert II projection schemes worked the best for this particular test problem. Tables I and II show the error norms for the various projection schemes. A larger number of points on the unit sphere can be selected at the cost of increasing computational time. We expect better agreement with the analytical solution as we increase the number of points on the unit sphere. The performance of the Eckert II projection was surprising. In Figure 13 we show the refinement of the Eckert II projection mesh with increasing points on the unit sphere. One possible explanation for the success of the Eckert II projection is the conservation of the surface area of the sphere. As we increase the number of points on the unit sphere, the projection area approach 4π as seen in Figure 12. In Figure 14 we show the refinement of the Sinusoidal projection mesh with increasing points on the unit sphere.

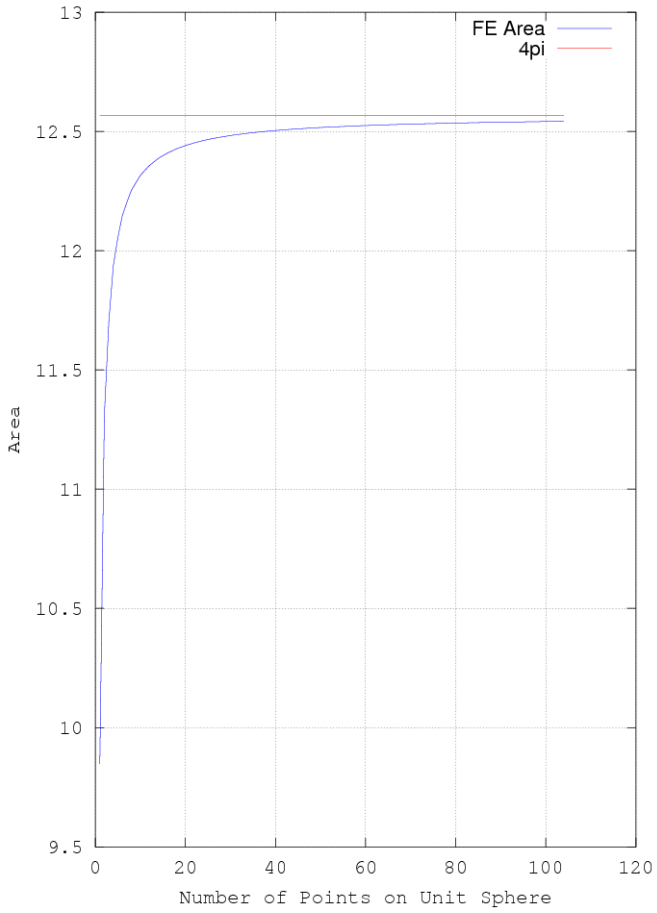

Fig. 12. Area of Eckert II Projection as Mesh is Refined

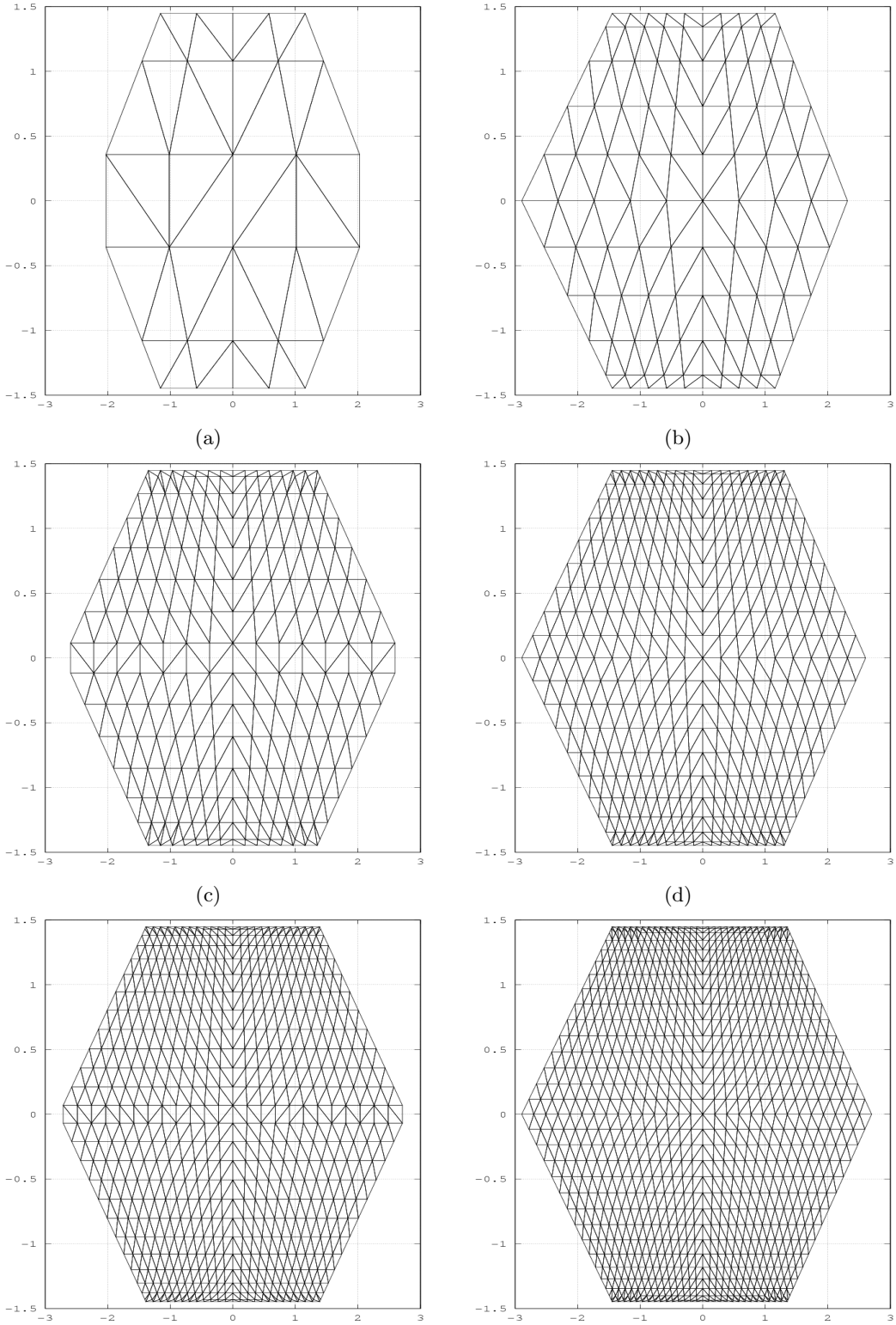

Fig. 13. Refinement of Unit Sphere Mesh using Eckert II Projection

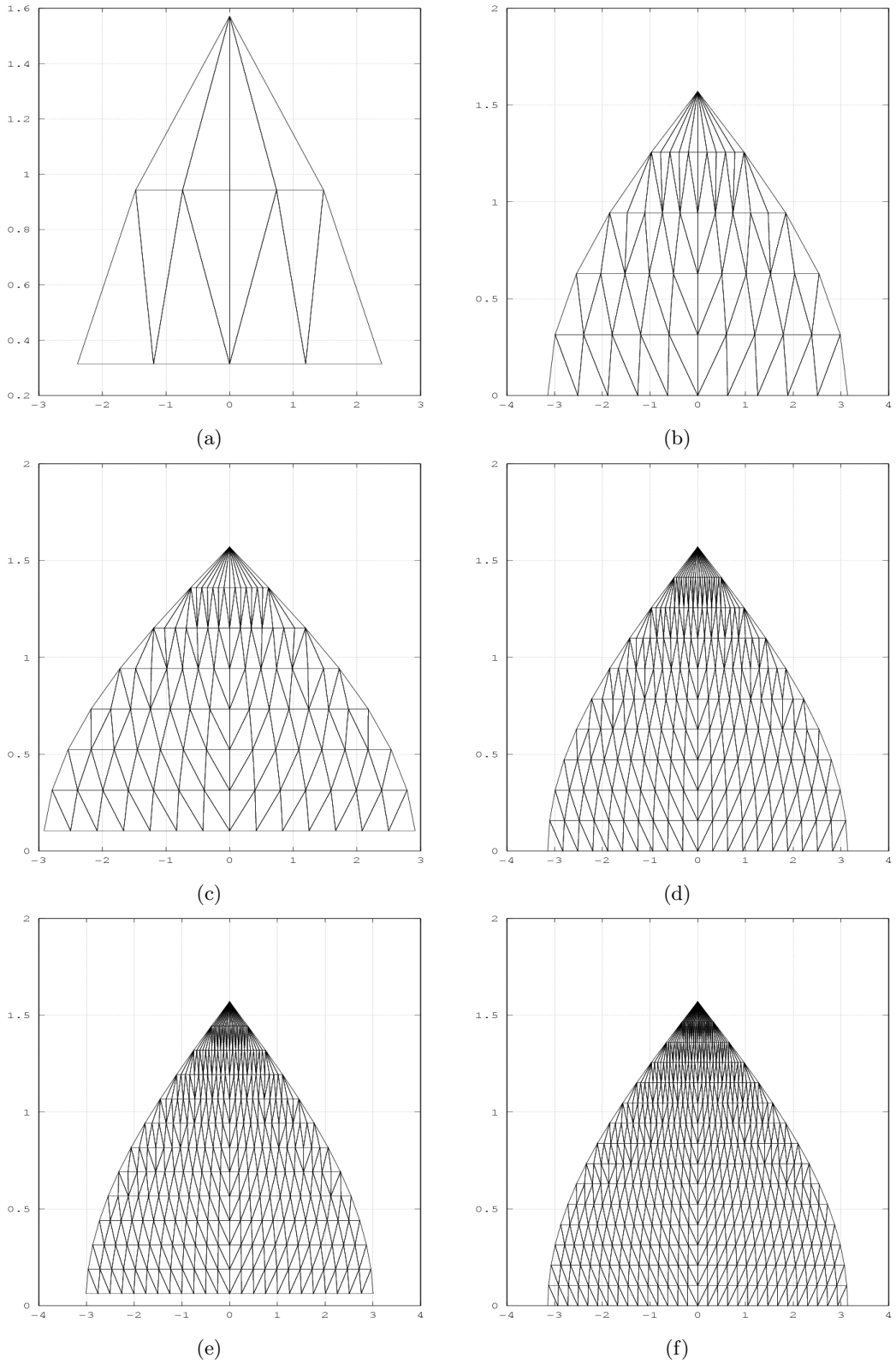

Fig. 14. Refinement of Unit Sphere Mesh using Sinusoidal Projection

IV. FUTURE WORK

A suite of problems should be created to test the Eckert II and Sinusoidal projection schemes. As the number of points on the sphere increase, the computational time increases substantially. It is necessary to develop schemes that allow for mesh refinement studies that do not take large amounts of time. In this study, the distribution of points on the unit sphere was uniform. It is of interest to see whether selecting points on the sphere using something like Lebedev quadrature improves the convergence properties of the mesh. It is also important to note that not all projection schemes conserve the 4π surface area of the unit sphere. It appears that preserving the area is important and all projection schemes used to transform the three-dimensional mesh should have this property.

ACKNOWLEDGMENTS

The author would like acknowledge the help and support of Clif R. Drumm, Shawn D. Pautz, and everybody else in Organization 1341 of Sandia National Laboratories. The practicum was made possible by the Department of Energy Computational Science Graduate Fellowship, provided under grant number DE-FG02-97ER25308. Sandia Sandia National Laboratories is a multimission laboratory managed and operated by National Technology and Engineering Solutions of Sandia, LLC., a wholly owned subsidiary of Honeywell International, Inc., for the U.S. Department of Energy's National Nuclear Security Administration under contract DE-NA0003525

REFERENCES

[1] J. P. Snyder, *Map Projections-A Working Manual*, vol. 1395, US Government Printing Office (1987).

[2] C. R. Drumm, "Multidimensional Electron-Photon Transport with Standard Discrete Ordinates Codes," *Nuclear Science and Engineering*, **127**, *1*, 1 (1997).

[3] S. D. Pautz, C. Drumm, W. C. Fan, and C. D. Turner, "A Discontinuous Phase-Space Finite Element Discretization of the Linear Boltzmann-Vlasov Equation for Charged Particle Transport," *Journal of Computational and Theoretical Transport*, **43**, *1-7*, 128 (2014).

[4] B. Wienke, "Transport Equation in Modified Eulerian Coordinates," *The Physics of Fluids*, **17**, *6*, 1135 (1974).

[5] C. R. Drumm, W. C. Fan, and S. D. Pautz, "Phase-Space Finite Elements in a Least-Squares Solution of the Transport Equation," , Sandia National Laboratories (SNL-NM), Albuquerque, NM (United States) (2013).